

Effect of phosphate on the adsorption of Cu and Cd on natural hematite

Wei Li, Shuzhen Zhang *, Wei Jiang, Xiao-quan Shan

Key Laboratory of Environmental Chemistry and Ecotoxicology, Research Center for Eco-Environmental Sciences, Chinese Academy of Sciences, P.O. Box 2871, Beijing 100085, China

Received 5 July 2005; received in revised form 11 October 2005; accepted 17 October 2005
Available online 1 December 2005

Abstract

Interactions between anions and cations are important to understand the chemical processes of pollutants in environment. In this study, batch experiments were carried out to investigate the simultaneous adsorption of Cu and Cd on hematite as affected by phosphate. Phosphate pretreatment suppressed the maximum adsorption of Cu and Cd on hematite and moved the adsorption pH edges to a higher pH range. Phosphate application time had a marked impact on Cu and Cd adsorption and longer contact time resulted in more reduction of Cu and Cd adsorption. Results of back-titration, Fourier transform infrared (FTIR) spectroscopy study and ionic strength effect on the adsorption revealed that Cu and Cd were adsorbed on hematite mainly through the inner-sphere complex formation mechanism and phosphate treatment reduced the inner-sphere adsorption sites, thus decreasing Cu and Cd adsorption on hematite.

© 2005 Elsevier Ltd. All rights reserved.

Keywords: Cu; Cd; Adsorption/Desorption; Phosphate; Hematite

1. Introduction

Copper (Cu) and Cadmium (Cd) are two typical potential hazardous trace metals in the environment. They may accumulate in soils due to agriculture application of sewage sludge and fertilizers, and/or through land disposal of metal-contaminated municipal and industrial wastes. Concentrations of heavy metals in soil solution, which are largely related to their mobility, toxicity and bioavailability are most likely controlled by adsorption–desorption reactions on the surface of soil colloidal materials (Brummer et al., 1988; Backes

et al., 1995; McLaren et al., 1998). Phosphate is an important nutrient element in soil. Phosphate in soil may affect the chemical reactions of metals on mineral surfaces. Recent studies (Traina and Laperche, 1999; Cao et al., 2002) indicated that phosphate minerals, such as apatite, could sequester heavy metals, metalloids and radionuclide through adsorption and/or the formation of secondary PO_4^{3-} precipitates, which remained stable under a wide range of geochemical conditions. Therefore, it is necessary to examine the influence of phosphate on the reactions of heavy metals on the surface of soil minerals.

Interactions between anions and cations were highly concerned by geochemists and environmental scientists. Phosphate has been intensively investigated as the co-ligand and was usually reported to have a positive effect on the heavy metal adsorption. Diaz-Barrentos et al.

* Corresponding author. Tel.: +86 10 6849683/6849329; fax: +86 10 62923563.

E-mail address: szzhang@mail.rcees.ac.cn (S. Zhang).

(1990) found that phosphate increased the Zn adsorption on lepidocrocite and explained it as the results of the decrease in electrostatic potential near the solid surface by phosphate. By using the CD-MUSIC surface complex model, Venema et al. (1997) investigated Cd adsorption on goethite in the presence of phosphate and revealed that phosphate enhanced the Cd loading. Collins et al. (1999) employed extended X-ray absorption fine structure spectroscopy (EXAFS) to investigate Cd adsorption in the Cd–phosphate–goethite tannery system, there was no evidence for the formation of Cd–phosphate complex. They interpreted the enhancement effect of phosphate as the electrostatic interaction mechanism. Wang and Xing (2002, 2004) treated goethite with phosphate to study the mutual effects of PO_4^{3-} and Cd^{2+} and observed that phosphate moved the Cd adsorption pH edge to a lower pH, which confirmed phosphate had a positive effect on Cd adsorption. Cheng et al. (2004) found that at low pH the adsorption of U (VI) on goethite-coated sand was increased in the presence of phosphate. However, the reduction of Cd adsorption in the presence of phosphate in some soils has also been reported (Krishnamurti et al., 1999). Additionally, Lee and Doolittle (2002) found that Cd adsorption tended to decrease in the presence of monopotassium phosphate but to increase in the presence of dipotassium phosphate in soils.

These investigations gave us valuable information about the effect of phosphate on the heavy metal adsorption. But very limited information is available about metal adsorption on hematite, the second most common Fe oxide in soils after goethite. Reactions of heavy metals on hematite are valuable to understand the behaviors of heavy metals in soil. On the other hand, interaction between phosphate and soil minerals always occurs before the introduction of exogenous heavy metals to soil. Therefore, sorption of heavy metals on hematite pretreated with phosphate is more close to the reactions in the natural environment.

In this work, a hematite separated from natural ore was pretreated by phosphate and used as the sorbent for Cu and Cd adsorption. The surface characteristics of hematite as affected by phosphate application and the effects of phosphate application on Cu and Cd sorption on hematite were investigated.

2. Materials and methods

2.1. Hematite preparation

Hematite ($\alpha\text{-Fe}_2\text{O}_3$) used in this work was a National Standard Matter (No. YSBCH702-94) separated from natural ore, which was supplied by the Chinese Central Iron & Steel Research Institute. Energy dispersive X-ray (EDX) (Zeiss DSM 950, Germany) analysis confirmed

that the sample was $\alpha\text{-Fe}_2\text{O}_3$ and had the following composition of 64.9% TFe, 0.52% Al_2O_3 , 3.95% SiO_2 and 0.16% MnO.

Hematite was saturated by a 0.5 M NaCl solution, and then washed by Mili-Q water until no Cl^- ions could be detected. Then it was dried at 60 °C and ground to pass a 100-mesh sieve, labeled as untreated sample (UT). Several portions of hematite (0.5 g) were shaken with 30 ml of 1 mM of Na_2HPO_4 in a rotary shaker for 1 h. The samples were washed three times with Mili-Q water to remove excess HPO_4^{2-} ions and then dried and ground again, labeled as shorter time treated sample (ST). Another several portions were treated in the same way for 24 h, labeled as longer time treated sample (LT).

2.2. Sample surface characteristics

The cation exchange capacity (CEC) of the solids was determined by Ba–Mg exchange without pH buffering. The specific surface area (SSA) of the solids was determined by a five-point N_2 Brunauer–Emmett–Teller (BET) gas adsorption isotherm method. Electrophoretic mobility as a function of pH was determined by microelectrophoresis using a Zeta-Meter 3.0 system. The EMs of oxide suspensions containing 0.02% solid in 0.01 M NaNO_3 were determined at various pH values. The pH_{PZC} was obtained by interpolating the data to zero EM (Goldberg and Johnston, 2001).

Fourier transform infrared (FTIR) spectra were obtained with a Nicolet Nexus 670 FTIR spectrometer and a horizontal ATR attachment (Squareco) using a trapezoidal-shape ZnSe internal reflection element with nine reflection at a 45° angle. The measured pathlength was 20 μm at 1630 cm^{-1} based on the molar absorptivity of water. The ZnSe internal reflection element did not permit observation of IR bands below 750 cm^{-1} . Spectra were obtained at a resolution of 4 cm^{-1} with each spectrum corresponding to the coaddition of 128 scans using a medium-band liquid N_2 cooled MCT detector. IR spectra of each sample were obtained as dry samples in KBr pellets corresponding to 3 mg of sample in ≈ 250 mg of spectral grade KBr.

To determine the amount of OH^- released into solution during the sorption of phosphate, back-titration technique (Martin and William, 1993) was employed. The procedure for back-titration was performed as follows: duplicate 2 g samples of hematite were equilibrated with 40 ml electrolyte solution (0.01 M NaNO_3) for 24 h, and the pH of the suspension was adjusted to 4.0 with 0.1 M HNO_3 for every 3 h during the equilibrium. Titration was carried out with 0.01 M NaOH automatically at the rate of 0.05 ml min^{-1} from pH 4.0 to 10.0. The surface charge due to hydroxyl ions consumed was calculated by subtracting the OH^- consumed from sample suspension titration at the same pH.

2.3. Adsorption experiment

Batch technique was employed to conduct the adsorption/desorption experiments. Adsorption isotherm was measured by preparing a series of initial concentrations of equal amount of Cu and Cd in centrifuge tubes with each tube having the same solid suspension density (5 g l^{-1}) (Pan and Liss, 1998). Adsorption suspensions were generated using 0.01 M NaNO_3 to maintain constant ionic strength. Addition of 0.1 M NaOH or 0.1 M HNO_3 was used to maintain a constant pH of 6 during the course of the experiment. The tubes were capped and shaken for 24 h at 25°C . After equilibration, solids were removed by centrifugation and filtrated through a $0.2 \mu\text{m}$ membrane filter. Filtered supernatants were served for analysis.

Adsorption curves (edges) were conducted as follows: a large number of samples (at least 20) with the same initial metal concentration ($10 \mu\text{M}$) at various pH values rather than employing duplicates or triplicates at a fixed pH, due to the extreme difficulty to achieve the same pH for replicates. Other conditions, such as ion strength and solid suspension density, were the same as in the isotherm experiments. Ionic strength effect was carried out with the same procedure as the adsorption pH edges by just changing the background electrolyte concentrations of 0.001 , 0.01 and 0.1 M .

2.4. Desorption experiment

Desorption studies were initiated by replacing the supernatant liquid with metal-free electrolyte solution in order to lower the solution-phase adsorbate concentration. Operation was conducted at 25°C by removing the adsorption equilibrium supernatant solution after centrifugation, replacing the solution with an equal volume of 0.01 M NaNO_3 background solution, adjusting the pH to 6, and then shaking for 24 h.

2.5. Analysis methods

Cu and Cd were analyzed by ICP–OES (Optima 3300 DV, Perkin–Elmer, Norwalk, CT, USA), equipped with a 40 MHz , free-running RF generator and an array detector allowing for the simultaneous determination of the elements using two different wavelengths. Multi-level standards (National Research Center for Certified

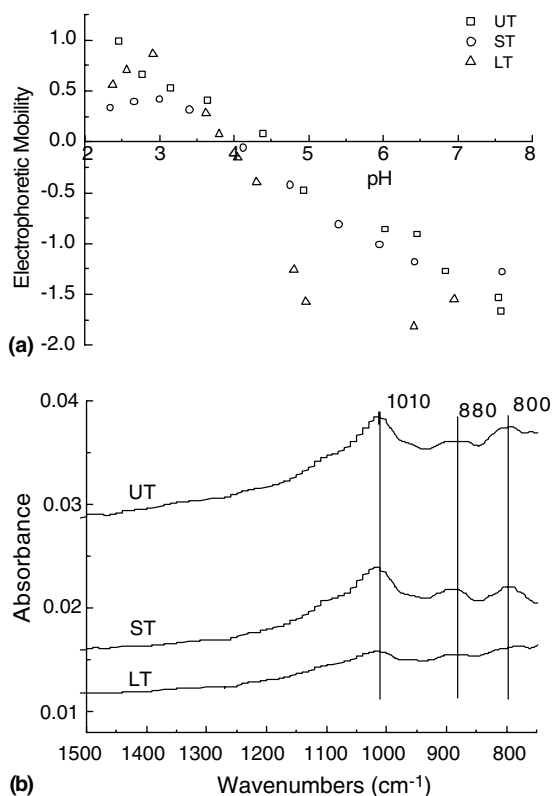


Fig. 1. Surface characteristics of hematite samples. (a) Electrophoretic mobility as a function of pH. (b) FTIR spectra; UT: untreated sample; ST: 1 h treated sample; LT: 24 h treated sample.

Reference Materials, Beijing, China) and determination samples were prepared in 2% nitric acid. Phosphate was determined by using the molybdate blue method with a Perkin–Elmer Lambda 3 spectrophotometer at 670 nm . Solution pH was determined using a Fisher Scientific Accumet model 20 pH/conductivity meter. All reagents used were of analytical grade or better.

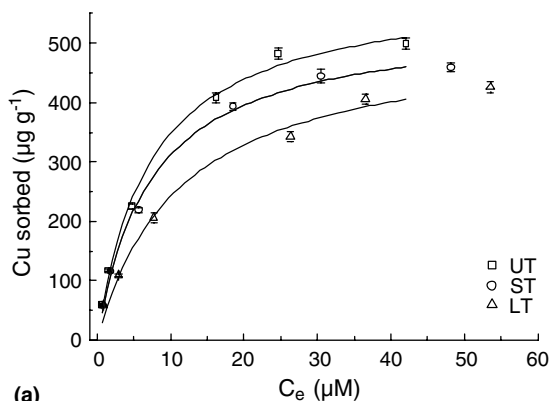
3. Results

3.1. Hematite properties

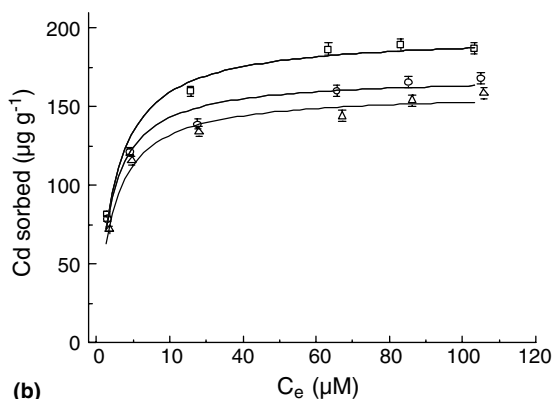
Some properties of the hematite with and without the phosphate pretreatment are listed in Table 1. In

Table 1
Surface characteristics of hematite samples with and without phosphate pretreatment

Sample	Treatment time	Phosphate binding ($\mu\text{mol g}^{-1}$)	BET surface area ($\text{m}^2 \text{g}^{-1}$)	CEC (cmol kg^{-1})	PZC	OH^{-1} released ($\mu\text{mol g}^{-1}$)
UT	0	0	20.53	66.71	4.51	0
ST	1 h	0.437	18.92	54.51	4.01	0.542
LT	24 h	0.631	18.08	37.20	3.82	0.982



(a)



(b)

Fig. 2. Adsorption isotherms of Cu and Cd. UT: untreated sample; ST: 1 h treated sample; LT: 24 h treated sample.

comparison, the SSA and CEC decreased with the increase in the phosphate adsorption time. Electrophoretic mobility decreased with the increase in pH and the point of zero charge (pH_{pzc}) of hematite decreased approximately with the increased phosphate coverage (Fig. 1(a)), which is consistent with the results of Huang (2004).

3.2. Adsorption isotherms

Fig. 2 presents the adsorption isotherms of Cu and Cd on the three samples (UT, ST, and LT) at pH 6. Langmuir equation was used to simulate the adsorption isotherm.

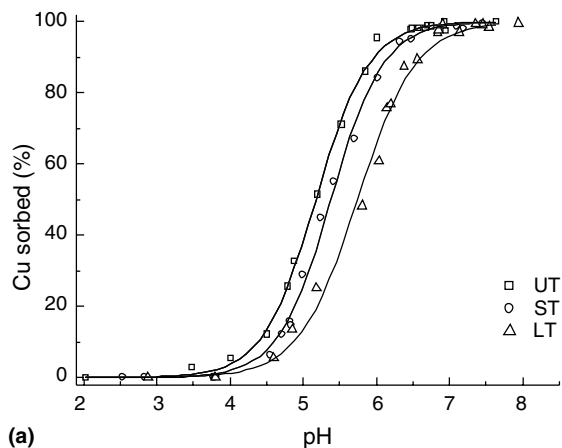
Parameters to quantify the adsorption process are listed in Table 2. The maximum adsorption capacities of Cu and Cd were in the order: $\text{UT} > \text{ST} > \text{LT}$. Pretreatment with phosphate suppressed the adsorption of Cu and Cd on hematite and such effect was more evident for the longer treatment sample (LT). The adsorption capacity ($\mu\text{g g}^{-1}$) of Cu is higher than that for Cd in all the samples, indicating that Cu has a relatively stronger affinity to hematite than Cd, because Cu has a smaller size of the hydrated radius than Cd.

Table 2
Langmuir equation parameters

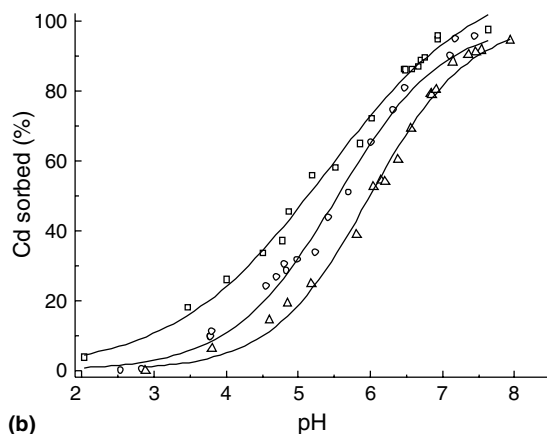
Metal ion	Sample	Phosphate pretreated time	Langmuir parameters		
			G_0 ($\mu\text{g g}^{-1}$)	b (μM)	r^2
Cu(II)	UT	0	578.03	6.89	0.9961
	ST	1 h	552.49	7.76	0.9959
	LT	24 h	512.82	11.2	0.9931
Cd(II)	UT	0	195.69	4.62	0.9761
	ST	1 h	185.19	4.67	0.9747
	LT	24 h	158.98	5.13	0.9779

3.3. Effect of pH and ionic strength

Copper adsorption by hematite was highly pH-dependent (Fig. 3(a)). Its adsorption increased to nearly 100% in a narrow pH range. The adsorption edge was markedly shifted to higher pH when hematite was pre-



(a)



(b)

Fig. 3. Effect of pH on the adsorption of Cu and Cd. UT: untreated sample; ST: 1 h treated sample; LT: 24 h treated sample.

treated with phosphate. The curve for the sample with longer treatment time (LT) shifted further than that for shorter time treated sample (ST), indicating the substantial reduction of Cu adsorption. Fig. 3(b) represents the adsorption of Cd, which is similar to Fig. 3(a). Within the pH range from 3 to 8, Cd adsorption followed the order: UT > ST > LT, which was in agreement with the results from the pH-constant adsorption (adsorption isotherms).

Fig. 4 shows the adsorption pH edges with solution ionic strength varied from 0.001 to 0.1 M NaNO₃. All the adsorption increased with increasing the solution pH and exhibited independence on ionic strength.

3.4. Desorption processes

Desorption experiments were performed for a better understanding of the adsorption processes. Fig. 5 shows that only a little Cu and Cd were released from phosphate treated samples, suggesting Cu and Cd were strongly adsorbed. The adsorption and desorption processes for Cu and Cd on the treated hematite are rather not coincided, which was referred to as desorption hysteresis. Hysteresis angles (the angle between adsorption and desorption isotherms, i.e. the angle BAC in Fig. 5(a)) were calculated to evaluate the adsorption

reversibility (Verburg and Baveye, 1994; Pan and Liss, 1998) and given in Fig. 5. According to the method by Verburg, only when hysteresis angle is smaller than 5°, the adsorption process can be considered as reversible. In this work, the hysteresis angle for Cu adsorption on ST is 24.9°, Cu on ST is 32.0°, Cd on ST 37.3° and Cd on LT 37.9°; each of them is much bigger than 5°, indicating the obvious irreversible adsorption of Cu and Cd on hematite with phosphate treatment.

4. Discussion

4.1. Surface characteristic changes as affected by phosphate pretreatment

Surface binding of phosphate on the LT was 0.6313 $\mu\text{mol g}^{-1}$ and bigger than that on the ST (Table 1), which was in agreement with the phosphate adsorption kinetics (Huang, 2004). Earlier studies (Hayes et al., 1988; Persson et al., 1996a,b; Huang, 2004) reported that phosphate was strongly adsorbed on hematite through an inner-sphere ligand exchange mechanism. Calculation results of back-titration showed the phosphate binding on LT released more OH⁻ than that on ST (Table 1). It suggested that the amount of hydroxyl on

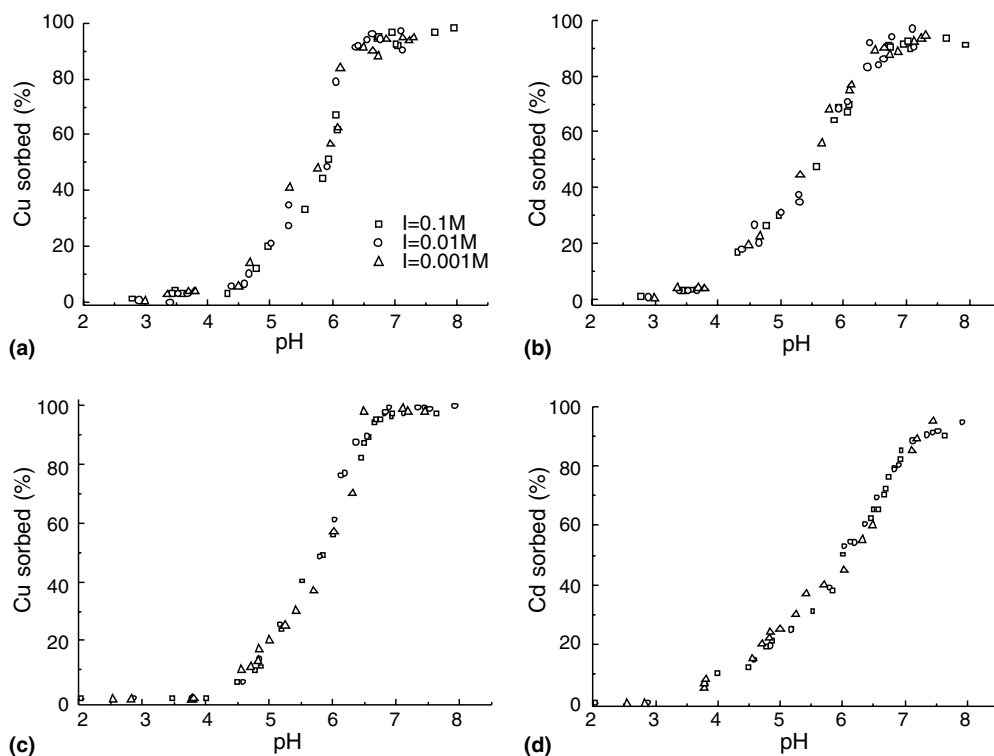


Fig. 4. Ionic strength effect on Cu and Cd adsorption. (a) Cu on ST; (b) Cd on ST; (c) Cu on LT; (d) Cd on LT.

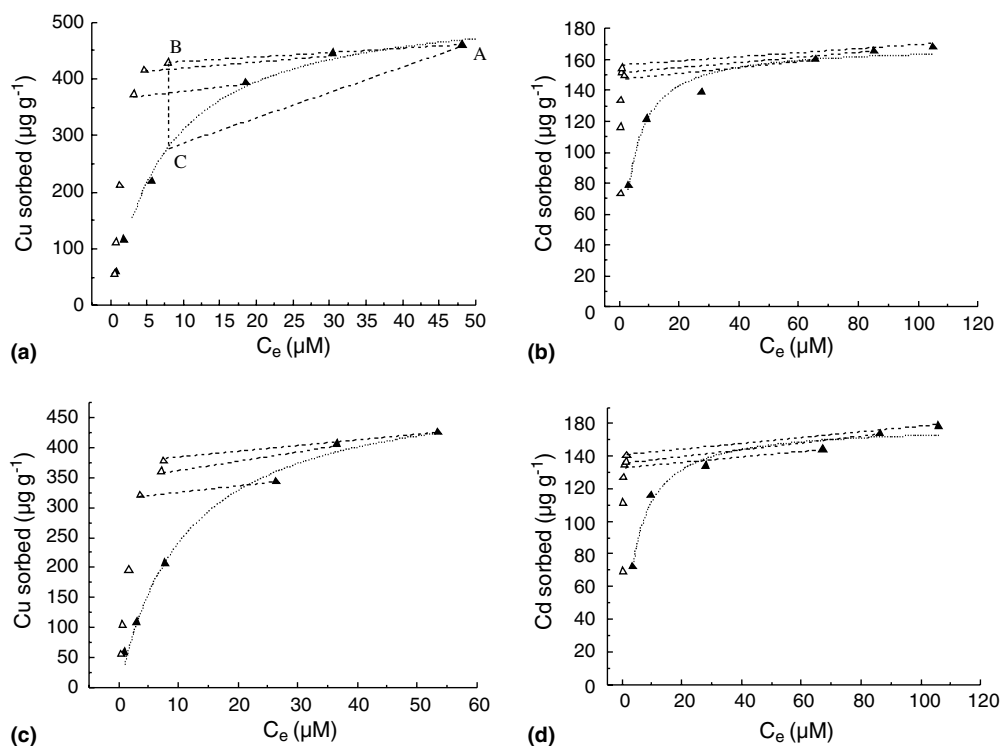


Fig. 5. Desorption isotherms of Cu and Cd. (▲) present the adsorption point; (△) present the desorption point. (a) Cu on ST; (b) Cd on ST; (c) Cu on LT; (d) Cd on LT.

the hematite surface decreased after phosphate pretreatment. FTIR spectroscopy also confirmed it since a weakening of the absorption band at about 1010 cm^{-1} , 880 cm^{-1} , and 800 cm^{-1} in the order $UT > ST > LT$ (Fig. 1(b)) was observed and these peaks were the evidence of Fe–O–H bending vibration by earlier literatures (Towe and Bradley, 1967; Russell, 1979).

4.2. Effect of phosphate pretreatment on the Cu and Cd adsorption

Both the pH-constant (isotherms) and the pH-dependent adsorptions showed that phosphate reduced Cu and Cd adsorption on hematite, and such effect existed across a wide pH (Fig. 3) and cation concentration ranges (Fig. 2). The results are inconsistent with the previous works (Venema et al., 1997; Collins et al., 1999; Wang and Xing, 2002; Wang and Xing, 2004), in which enhanced Cd adsorption on goethite by phosphate pretreatment or in the presence of phosphate were observed. The authors explained the reason as the phosphate adsorption increasing surface negative charges and consequently decreasing the electrostatic potential near the solid surface (Diaz-Barrantos et al., 1990; Collins et al., 1999; Wang and Xing, 2004). But some other studies (Davis and Leckie, 1978; Benjamin and Leckie, 1982) also reported that the complex ligands Cl^- and

$\text{S}_2\text{O}_3^{2-}$ reduced heavy metals uptake onto (hydr)oxides due to the competition for the adsorption sites.

Phosphate can occupy the inner-sphere adsorption sites ($\equiv\text{FeOH}$) on the mineral surface, decreasing the inner-sphere adsorption sites for heavy metals. On the other hand phosphate can also lower the surface electrostatic potential near the solid surface and therefore enhance the heavy metal uptake through outer-sphere complex. If Cu and Cd are adsorbed mostly as outer-sphere complexes, Cu and Cd adsorption could be enhanced by phosphate. Otherwise, their sorption would be suppressed when they mainly adsorbed through inner-sphere complex.

Our results (Fig. 5) indicated that the adsorption and desorption processes of Cu and Cd on hematite were irreversible, which was one of the characteristics of inner-sphere complex while outer-sphere complex was reversible (Sparks, 2002). Study of the ionic strength effects on adsorption was conducted consequently as another evidence to distinguish outer-sphere and inner-sphere complexes (Hayes et al., 1988). McBride (1997) indicated that ions forming inner-sphere surface complexes showed little ionic strength dependence and outer-sphere complexes would increase with increasing solution ionic strength. Fig. 4 showed Cu and Cd adsorption was independent on ionic strength, suggesting that they were mainly adsorbed on the inner-sphere

sites. Therefore, we can infer that phosphate decreases Cu and Cd adsorption on hematite mainly by occupying the inner-sphere adsorption sites. However, this description does not mean that the adsorption of Cu and Cd only occurs as inner-sphere complexes. The facts that with pH increase, the electrophoretic mobility of the hematite samples decreased caused by the amount of hydroxyl increase and the adsorption of Cu and Cd increased with pH suggested the interaction between anion and cation on the hematite surface.

5. Conclusions

The decreases of the maximum adsorption capacity and the substantial shifts of adsorption edges to higher pH indicate that phosphate treatment decreases Cu and Cd adsorption on hematite. Prolonging phosphate application time leads to more phosphate adsorbed and more significant suppression of Cu and Cd adsorption on hematite. Cu and Cd are adsorbed on hematite mainly through the inner-sphere complex formation mechanism. Phosphate adsorption reduces the inner-sphere sorption sites, therefore, decreasing Cu and Cd adsorption on hematite.

Acknowledgements

This work was funded by National Natural Science Foundation of China (Nos. 20377049 and 20237010).

References

- Backes, C.A., McLaren, R.G., Rate, A.W., Swift, R.S., 1995. Kinetics of cadmium and cobalt desorption from iron and manganese oxides. *Soil Sci. Soc. Am. J.* 59, 778–785.
- Benjamin, M.M., Leckie, J.O., 1982. Effects of complexation by Cl^- SO_4^{2-} and $\text{S}_2\text{O}_3^{2-}$ on adsorption behavior of Cd on oxide surfaces. *Environ. Sci. Technol.* 16, 162–170.
- Brummer, G.W., Gerth, J., Tiller, K.G., 1988. Reaction kinetics of the adsorption and desorption of nickel, zinc and cadmium by goethite. I. Adsorption and diffusion of metals. *J. Soil Sci.* 39, 37–51.
- Cao, X., Ma, L.Q., Chen, M., Singh, S.P., Harris, W.G., 2002. Impacts of phosphate amendments on lead bioavailability at a contaminated site. *Environ. Sci. Technol.* 36, 5296–5304.
- Cheng, T., Barnett, M.O., Roden, E.E., Zhuang, J., 2004. Effects of phosphate on uranium(VI) adsorption to goethite-coated sand. *Environ. Sci. Technol.* 38, 6059–6065.
- Collins, C.R., Ragnarsdottir, K.V., Sherman, D.M., 1999. Effect of inorganic and organic ligands on the mechanism of cadmium sorption to goethite. *Geochim. Cosmochim. Acta* 63, 2989–3002.
- Davis, J.A., Leckie, J.O., 1978. Effect of adsorbed complexing ligands on trace metal uptake by hydrous oxides. *Environ. Sci. Technol.* 12, 1309–1315.
- Diaz-Barrientos, E., Madrid, L., Contreras, M.C., Morillo, E., 1990. Simultaneous adsorption of zinc and phosphate on synthetic lepidocrocite. *Aust. J. Soil Sci.* 28, 549–557.
- Goldberg, S., Johnston, C.T., 2001. Mechanisms of arsenic adsorption on amorphous oxides evaluated using macroscopic measurements, vibrational spectroscopy, and surface complexation modeling. *J. Colloid Interf. Sci.* 234, 204–216.
- Hayes, K.F., Papelis, C., Leckie, J.O., 1988. Modeling ionic strength effects on anion adsorption at hydrous oxide/solution interfaces. *J. Colloid Interf. Sci.* 125, 717–726.
- Huang, X., 2004. Intersection of isotherms for phosphate adsorption on hematite. *J. Colloid Interf. Sci.* 271, 296–307.
- Krishnamurti, G.S.R., Huang, P.M., Kozak, L.M., 1999. Sorption and desorption kinetics of cadmium from soils: influence of phosphate. *Soil Sci.* 164, 888–898.
- Lee, J.H., Doolittle, J.J., 2002. Phosphate application impacts on cadmium sorption in acidic and calcareous soils. *Soil Sci.* 167, 390–400.
- Martin, D., William, H., 1993. Soil surface charge evaluation by back-titration: I. Theory and method development. *Soc. Soil. Sci. Am. J.* 57, 1222–1228.
- McBride, M.B., 1997. Critique of diffuse double layer models applied to colloid and surface chemistry. *Clays Clay Miner.* 45, 598–608.
- McLaren, R.G., Backs, C.A., Rates, A.W., Swift, R.S., 1998. Cadmium and cobalt desorption kinetics from soil clays: effect of sorption period. *Soil Sci. Soc. Am. J.* 62, 332–337.
- Pan, G., Liss, P.S., 1998. Metastable-equilibrium adsorption theory: I Theoretical. *J. Colloid Interf. Sci.* 201, 71–76.
- Persson, P., Lövgren, L., Sjöberg, S., 1996a. Competitive surface complexation of *o*-phthalate and phosphate on goethite (α -FeOOH) particles. *Geochim. Cosmochim. Acta* 60, 4385–4395.
- Persson, P., Nilsson, N., Sjöberg, S., 1996b. Structure and bonding of orthophosphate ions at the iron oxide-aqueous interface. *J. Colloid Interf. Sci.* 177, 263–275.
- Russell, J.D., 1979. Infrared spectroscopy of ferrihydrite: evidence for the presence of structural hydroxyl groups. *Clay Miner.* 14, 109–114.
- Sparks, D.L., 2002. *Environmental soil chemistry*. Academic Press, New York.
- Towe, K.M., Bradley, W.F., 1967. Mineralogical constitution of colloidal “Hydrous Ferric Oxides”. *J. Colloid Interf. Sci.* 24, 384–392.
- Traina, S.J., Laperche, V., 1999. Contaminant bioavailability in soils, sediments, and aquatic environments. *Proc. Nat. Acad. Sci.* 96, 3365–3371.
- Venema, P., Hiemstra, T., van Riemsdijk, W.H., 1997. Interaction of cadmium with phosphate on goethite. *J. Colloid Interf. Sci.* 192, 94–103.
- Verburg, K., Baveye, P., 1994. Hysteresis in the binary exchange of cations on 2:1 clay minerals: A critical review. *Clays Clay Miner.* 42, 207–220.
- Wang, K., Xing, B., 2002. Adsorption and desorption of cadmium by goethite pretreated with phosphate. *Chemosphere* 48, 665–670.
- Wang, K., Xing, B., 2004. Mutual effects of cadmium and phosphate on their adsorption and desorption by goethite. *Environ. Pollut.* 127, 13–20.